Raman and electron microscopic studies of $Si_{1-x}Ge_x$ alloy nanowires grown by chemical vapor deposition

Takahiro Kawashima[a)]
Advanced Devices Development Center, Matsushita Electric Industrial Co., Ltd., 3–1–1 Yagumo-Nakamachi, Moriguchi, Osaka 570-8501, Japan

Goh Imamura, Minoru Fujii, and Shinji Hayashi
Department of Electrical and Electronic Engineering, Graduate School of Engineering, Kobe University, 1-1 Rokkodai, Nada, Kobe 657-8501, Japan

Tohru Saitoh and Kazunori Komori
Image Devices Development Center, Matsushita Electric Industrial Co., Ltd., 3-1-1 Yagumo-Nakamachi, Moriguchi, Osaka 570-8501, Japan

(Received 31 July 2007; accepted 1 October 2007; published online 26 December 2007)

$Si_{1-x}Ge_x$ alloy nanowires (SiGeNWs) were grown by Au-catalyzed chemical vapor deposition and studied by Raman spectroscopy, transmission electron microscopy (TEM), and energy-dispersive x-ray spectroscopy (EDS) in TEM (TEM-EDS). The relationship between the growth parameters and the structure of the SiGeNWs was clarified by systematically changing the growth conditions over a wide range. Raman and TEM-EDS results demonstrated that the SiGeNWs consist of a lower Ge composition core and a higher Ge composition shell epitaxially grown on the surface of the core. The effects of oxidation on the structure of the SiGeNWs were studied. It was found that oxidation leads to segregation of the Ge atoms at the interface between the SiGeNWs and SiO_2, which in turn results in a large inhomogeneity in Ge composition. Oxidation at a very low rate in a diluted oxygen gas atmosphere is required to avoid the formation of Ge particles and minimize the inhomogeneity.
© *2007 American Institute of Physics*. [DOI: 10.1063/1.2817619]

I. INTRODUCTION

In recent years, semiconductor nanowires (NWs) have attracted significant attention due to their unique electronic properties and possible device applications as transistors,[1,2] chemical sensors,[3,4] and light-emitting devices.[5,6] Among the different kinds of semiconductor NWs, group IV semiconductor NWs such as Si and Ge NWs (SiNWs and GeNWs) have been the most widely studied because of their high compatibility with conventional complementary metal-oxide semiconductor (CMOS) technology. Nanowires of $Si_{1-x}Ge_x$ alloy (SiGeNWs) are also potentially very useful materials, since their energy band gap can be modulated within the wire and their electronic properties can be tailored over an extended range. Recently, several groups have reported the synthesis of SiGeNWs by a vapor-liquid-solid (VLS) process.[7,8] Wu *et al.* synthesized $Si/Si_{1-x}Ge_x$ superlattice nanowires using a hybrid pulse laser ablation/chemical vapor deposition (PLA-CVD) process and demonstrated single crystalline nanowires with a longitudinal $Si/Si_{1-x}Ge_x$ superlattice structure.[7] Core-shell type SiGeNWs with different Ge compositions between the core and the shell have also been fabricated.[8]

Despite the possible applications of SiGeNWs in future electronic devices, research on the growth mechanism is still rather limited, and thus the growth parameters and strategies for the fabrication of high-quality SiGeNWs are not fully elucidated. The mechanism of the VLS growth of SiGeNWs is considered to be more complex than those of SiNWs and GeNWs, since different kinds of source gases are mixed during growth, and the solubility of Si and Ge in Au catalysts is different. Furthermore, because of these different solubilities, the growth mechanism is believed to depend on the composition.

In this study, we grew SiGeNWs by systematically changing the growth parameters and studied them by Raman spectroscopy and transmission electron microscopy (TEM) combined with energy-dispersive x-ray spectroscopy (EDS). The purpose of this work is to clarify the parameters that control the shape, crystallinity, and homogeneity of the Ge composition, etc., of SiGeNWs and also clarify their growth mechanism. We show that Ge composition and the shapes of SiGeNWs depend strongly on the growth temperature as well as the partial pressure of source gases. Furthermore, our results demonstrate that SiGeNWs consist of a lower-Ge composition core and a higher-Ge composition shell epitaxially grown on the core. We also studied how the structure of SiGeNWs is modified by oxidation, and demonstrated that the oxidation of SiGeNWs leads to the segregation of Ge atoms at the interface between SiGeNWs and SiO_2: this segregation results in a large inhomogeneity in the Ge composition.

II. EXPERIMENTS

SiGeNWs were synthesized via VLS growth using a cold-wall infrared (IR) lamp-heated chemical vapor deposition (CVD) apparatus. To attach the catalysts to the Si substrates, thermally oxidized Si (100) wafers were first treated

[a)]Electronic mail: kawashima.takahiro@jp.panasonic.com.

 © 2007 American Institute of Physics

Author complimentary copy. Redistribution subject to AIP license or copyright, see http://jap.aip.org/jap/copyright.jsp

with oxygen plasma and dipped into 1 wt % solution of 3,5-diaminopentyltrimethoxysilane. The substrates were then dipped into a solution of gold (Au)-colloid (Tanaka Kikinzoku Co.) for 5–30 min. After drying, the substrates were loaded into the CVD chamber. The flow rate of the Si_2H_6 precursor, GeH_4 precursor and H_2 were 100–450, 100–450, and 0–1100 sccm (cubic centimeters per minute at STP), respectively, and the total pressure was about 0.2–1 Torr. The partial pressures of the Si_2H_6 and GeH_4 precursors were 0.002–0.008 and 0.003–0.016 Torr, respectively. The total pressure was controlled by changing the H_2 flow rate. The growth temperature was varied between 350 and 450 °C, and was monitored using a pyrometer. The growth duration was 10 min. To study the effects of oxidation on the structure of SiGeNWs, they were annealed in an oxygen atmosphere (about 1 atm) at 900–1100 °C for 2–6 min.

Raman measurements were carried out in a conventional 90° scattering configuration by using a triple monochromator (Spex 1877E) equipped with a charge-coupled device (CCD) detector. The excitation source was the 514.5 nm line of an argon (Ar) ion laser. The laser power applied to the sample was about 3 mW. At this power level, no significant shift or broadening of the Raman spectra by laser heating was observed. The signal from the Si substrate was not observed because of the high density of the SiGeNWs grown on it.

The morphology of the SiGeNWs was studied by a scanning electron microscope (SEM) (Hitachi, S-4000) and a transmission electron microscope (TEM) (JEOL JEM-4000DX) operated at 400 kV. For the TEM observations, the SiGeNWs were separated from the growth substrates by ultrasonication in ethanol, and the solvent containing the SiGeNWs was then dropped onto a microgrid. The crystallinity of the SiGeNWs was also studied by TEM. The chemical compositions of the SiGeNWs, especially the Ge distribution within the SiGeNWs, were analyzed using energy-dispersive x-ray spectroscopy (EDS) in TEM (TEM-EDS). The electron beam diameter for the TEM-EDS measurements was about 1–2 nm. To quantitatively determine the chemical compositions by TEM-EDS, we used $Si_{1-x}Ge_x$ thin films (100 nm in thickness) with three different x (19.6, 24.9, and 30.1 at %) values, epitaxially grown on Si substrates using the same apparatus as the reference samples. The chemical composition of the reference $Si_{1-x}Ge_x$ thin films was determined by x-ray diffraction (XRD).

III. RESULTS AND DISCUSSION

A. Raman scattering studies of as-grown SiGeNWs

Figure 1 shows plan-view SEM images of the SiGeNWs prepared at different GeH_4 partial pressures (flow rates), i.e., 0.003 (100 sccm), 0.007 (200 sccm), and 0.01 (300 sccm) Torr in Figs. 1(a)–1(c), respectively. The other growth parameters are fixed [Si_2H_6 partial pressure (flow rate): 0.002 Torr (100 sccm), H_2 flow rate: 1100 sccm, growth temperature: 450 °C, growth duration: 10 min]. In all the samples, the diameter and the length of the SiGeNWs are almost the same and are ~50–100 nm and ~7 μm, respectively, while the shape is significantly different. As can be seen in Fig. 1, the shape becomes more conelike when the SiGeNWs are grown at a higher GeH_4 partial pressure. To find out whether the change in shape is chiefly caused by the different ratios of the Si_2H_6 and GeH_4 partial pressures or different total gas pressure, which changes from 0.2 to 0.5 Torr due to the change in the GeH_4 flow rate, we studied a large number of samples prepared under different conditions. Our results show that, within the present growth condition range, whether the wires become cylinderlike or conelike depends most strongly on the ratio of the Si_2H_6 and GeH_4 partial pressures but depends little on the total pressure. Therefore, in the following, we fixed the partial pressure of Si_2H_6 (0.002 Torr) and changed only that of GeH_4 (0.003–0.01 Torr) to control the shape. The ratio of the GeH_4 partial pressure with respect to the Si_2H_6 and GeH_4 partial pressures [$GeH_4/(GeH_4+Si_2H_6)$] is changed from 0.6 to 0.83. Hereafter, we will use the value of $GeH_4/(GeH_4+Si_2H_6)$ to represent the samples.

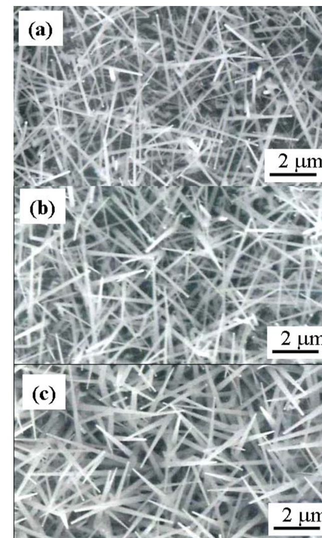

FIG. 1. Plan-view SEM images of SiGeNWs grown with the GeH_4 gas partial pressures (flow rates) of (a) 0.003 Torr (100 sccm); (b) 0.007 Torr (200 sccm); and (c) 0.01 Torr (300 sccm). Other growth parameters are fixed. The ratio of GeH_4 partial pressure with respect to GeH_4 and Si_2H_6 partial pressures [$GeH_4/(GeH_4+Si_2H_6)$] in (a), (b), and (c) is 0.6, 0.78, and 0.83, respectively. The growth temperature is 450 °C.

Figure 2(a) shows the Raman spectra of the SiGeNWs. $GeH_4/(GeH_4+Si_2H_6)$ is changed from 0.6 to 0.83. Three major peaks at 500–520, 400–410, and 280–290 cm^{-1} correspond to optical phonons caused by the motions of adjacent Si-Si, Si-Ge, and Ge-Ge pairs, respectively.[9] The peak around 420 cm^{-1} is assigned to a local vibration mode of the Si-Si pairs modulated by the adjacent Ge atoms.[10] We see that the Ge-Ge and Si-Ge modes grow with increasing $GeH_4/(GeH_4+Si_2H_6)$. This indicates that, similar to the epitaxial growth of $Si_{1-x}Ge_x$ thin films, Ge composition can be controlled by $GeH_4/(GeH_4+Si_2H_6)$ in SiGeNWs. The Ge composition can also be controlled by the growth temperature. In Fig. 2(b), the growth temperature is changed from 350 to 450 °C and other growth parameters are fixed. The intensity of the Ge-Ge mode with respect to the Si-Si mode is greater when the growth temperature is higher.

In $Si_{1-x}Ge_x$ thin films epitaxially grown on Si substrates, the Ge composition dependence on the frequencies of Si-Si,

Author complimentary copy. Redistribution subject to AIP license or copyright, see http://jap.aip.org/jap/copyright.jsp

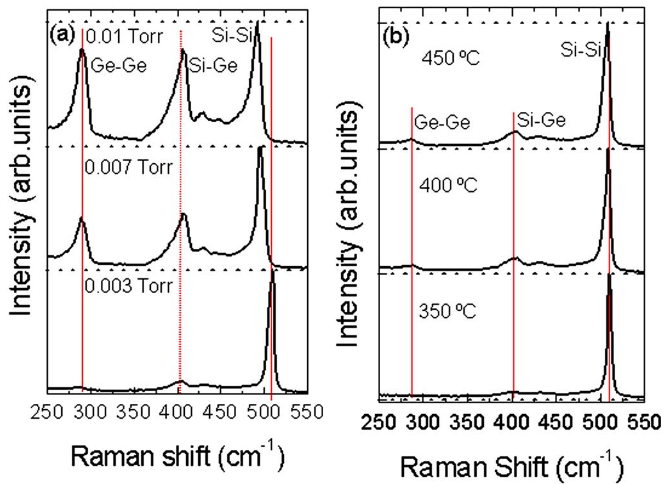

FIG. 2. (Color online) Raman spectra of SiGeNWs. (a) GeH_4 gas partial pressure is changed (0.003, 0.007, and 0.01 Torr, $GeH_4/(GeH_4+Si_2H_6)$ =0.6, 0.78, and 0.83), while other growth parameters are fixed. Growth temperature is 450 °C. (b) Growth temperature is changed (350, 400, and 450 °C), while other parameters are fixed. The partial pressures of GeH_4 and Si_2H_6 are 0.003 and 0.002 Torr, respectively, and thus $GeH_4/(GeH_4+Si_2H_6)$ is 0.6.

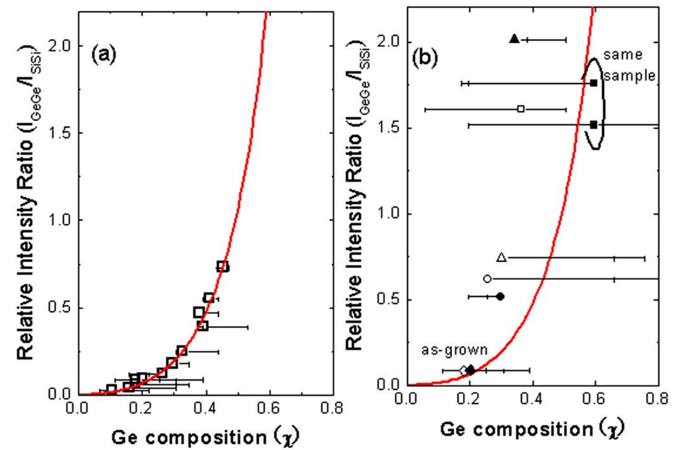

FIG. 3. (Color online) (a) Relative intensities of Si-Si and Ge-Ge Raman modes as a function of Ge composition determined from the shifts of Raman peaks. The data obtained for SiGeNWs grown at different temperatures (350–450 °C) and different ratios of GeH_4 and Si_2H_6 partial pressures [$GeH_4/(GeH_4+Si_2H_6)$=0.6, 0.78, and 0.83] are summarized. The solid curve is the result of fitting by Eq. (4). Ge composition is estimated from Eqs. (1)–(3). Ge composition obtained from Eq. (1) is represented by symbols (□) and those from Eqs. (2) and (3) by error bars. (b) The same data for SiGeNWs after oxidation. The data of the samples grown at different temperatures: 350 °C (open symbol) and 450 °C (filled symbol), are shown. Other growth parameters are fixed [$GeH_4/(GeH_4+Si_2H_6)$=0.6]. The oxidation temperatures are 900 °C (○●), 1000 °C (△▲) to 1100 °C (□■).

Si-Ge, and Ge-Ge modes was empirically obtained by taking into account the strain exerted from the Si substrates.[9] In the SiGeNWs in the first approximation, the strain is relieved. We thus try to estimate the Ge composition from the Raman peak frequencies by using the relations under strain-free conditions,[9]

$$\omega_{SS} = 520.2 - 62\chi, \tag{1}$$

$$\omega_{SG} = 400.5 + 14.2\chi, \tag{2}$$

$$\omega_{GG} = 282.5 + 16\chi, \tag{3}$$

where ω_{SS}, ω_{SG}, and ω_{GG} are the frequencies of the Si-Si, Si-Ge, and Ge-Ge modes, respectively, and x is the Ge composition. Figure 3 shows the intensity ratio of the Ge-Ge and Si-Si modes as a function of the Ge composition (x) estimated from Eqs. (1)–(3) for (a) as-grown and (b) oxidized SiGeNWs. In ideal cases, x obtained from the three Raman modes agrees perfectly. However, in the present SiGeNWs, the values scatter over a rather wide range for some samples. In Eqs. (1)–(3), the frequency of the Si-Si mode depends most strongly on Ge composition, and thus is most reliable in obtaining the composition, especially in the range where the Raman intensities of Ge-Ge and Si-Ge modes are very weak due to the small Ge composition. Therefore, in Fig. 3, x obtained from Eq. (1) is represented by symbols (□) and those from Eqs. (2) and (3) by error bars.

In Fig. 3(a), the data obtained for the SiGeNWs grown at different growth temperatures (350–450 °C) and different $GeH_4/(GeH_4+Si_2H_6)$ (0.6–0.83) are summarized. We can see that the error bars are rather large in some samples. The large error bars suggest that the Ge composition is not uniform within the SiGeNWs and it cannot be expressed as a single value. This will be confirmed later by TEM-EDS. It should be noted here that, despite the composition distribution, the x values estimated from Eq. (1) [□ in Fig. 3(a)] agree in most cases with those obtained from EDS and Rutherford backscattering (RBS) spectroscopy within an accuracy of 5 at %. Therefore, Raman scattering is still useful for roughly estimating the Ge composition of as-grown SiGeNWs, and x obtained from the Si-Si mode frequency probably represents the average Ge composition. This conclusion is not applicable to oxidized SiGeNWs, as discussed later.

If we assume a random mixing of Si and Ge in the $Si_{1-x}Ge_x$ alloy, the fractions of nearest-neighbor Ge atoms, those of Si atoms, and those of nearest-neighbor Si-Ge pairs are x^2, $(1-x)^2$, and $2x(1-x)$, respectively.[11] Since the scattering intensity of each of the three Raman modes should depend linearly on the fraction of pairs of atoms of each type, the intensity ratio of the modes is expected to vary with the Ge composition as[11]

$$I_{GG}/I_{SS} = A\frac{\chi^2}{(1-\chi)^2}, \tag{4}$$

where I_{SS} and I_{GG} are the scattering intensities of the Si-Si and Ge-Ge modes, respectively, and A is a fitting parameter that must be determined experimentally for each wavelength and may vary weakly with the alloy composition. The solid curve in Fig. 3(a) is the result of the fitting of the data by Eq. (4). For the fitting, the Ge compositions are assumed to be those obtained from Eq. (1), i.e., □ in Fig. 3(a). We can see that the data obey nearly perfectly the relation in Eq. (4). This confirms that the SiGeNWs are indeed random alloys on the scale of Raman measurements and not a mixture of Si and Ge crystals. Furthermore, the nearly perfect fitting supports the validity of Eq. (1) in estimating the Ge composition of as-grown SiGeNWs.

Author complimentary copy. Redistribution subject to AIP license or copyright, see http://jap.aip.org/jap/copyright.jsp

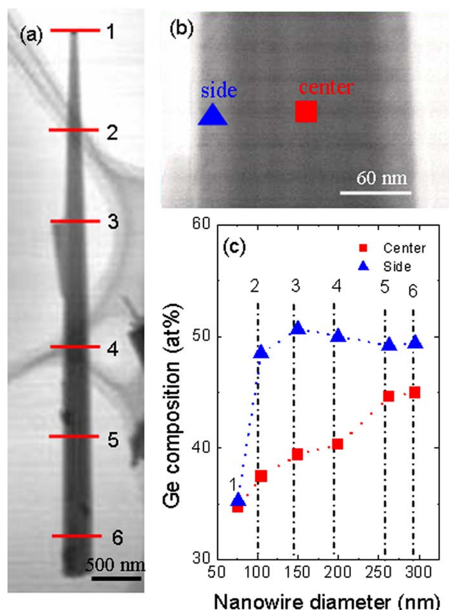

FIG. 4. (Color online) (a) Low-magnification TEM image of a SiGeNW. The partial pressures (flow rates) of GeH_4 and Si_2H_6 are 0.007 (200 sccm) and 0.002 Torr (100 sccm), respectively $[GeH_4/(GeH_4+Si_2H_6)=0.78]$, and the growth temperature is 450 °C. The numbers represent positions where Ge composition is measured by TEM-EDS. (b) High-magnification TEM image of a SiGeNW around the line 3 in (a). ■ and ▲ represent positions where TEM-EDS observations are made. (c) Ge composition measured at the center (■) and the peripheral (▲) regions of a SiGeNW as a function of nanowire diameter. The numbers correspond to those in (a) and the symbols correspond to those in (b).

B. TEM studies of as-grown SiGeNWs

In CVD growth of $Si_{1-x}Ge_x$ thin films, the addition of a Ge precursor, i.e., GeH_4 gas, is known to enhance the growth rate, i.e., to decrease the growth temperature due to complex interactions between source gases and the low pyrolysis character of GeH_4 gas.[12] The low pyrolysis temperature of GeH_4 results in a substantially lower growth temperature of GeNW (~260 °C) than that of SiNWs.[13] In the VLS growth of SiGeNWs, the low pyrolysis temperature of GeH_4 causes conformal deposition of the $Si_{1-x}Ge_x$ layer on the sidewall, which is considered to cause the growth of conelike-shaped NWs.[14] The formation of conelike-shaped SiGeNWs in the present work suggests a similar growth process. To study the mechanism of the formation of cone-shaped SiGeNWs in more detail, the Ge composition distribution in SiGeNWs was studied by TEM and TEM-EDS. Figure 4 shows the results of TEM-EDS analyses of an as-grown SiGeNW $[GeH_4/(GeH_4+Si_2H_6):0.78]$. Figure 4(a) shows a low-magnification TEM image in which we can clearly see a conelike SiGeNW. The lines with numbers in Fig. 4(a) represent the positions where the EDS measurements are made. Figure 4(b) shows a high-magnification TEM image around position 3 in Fig. 4(a). TEM-EDS measurements are performed at the center (■) and the peripheral (▲) regions. The Ge compositions of the center and the peripheral regions are 39.4 and 50.7 at %, respectively. The same measurements are performed at 6 positions, labeled from 1 to 6 in Fig. 4(a). The results are summarized in Fig. 4(c) as a function of NW diameter. In all the positions, Ge composition is higher in the

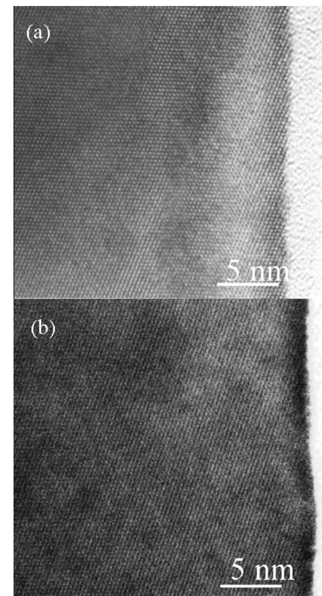

FIG. 5. High-resolution TEM images of (a) top (catalyst side) and (b) bottom (substrate side) of an as-grown SiGeNW. The partial pressures (flow rates) of GeH_4 and Si_2H_6 are 0.007 (200 sccm) and 0.002 Torr (100 sccm), respectively $[GeH_4/(GeH_4+Si_2H_6)=0.78]$, and the growth temperature is 450 °C.

peripheral regions than in the central regions. This means that the SiGeNW has a core-shell structure with a low-Ge composition $Si_{1-x}Ge_x$ core covered by a high-Ge composition $Si_{1-x}Ge_x$ shell. It is highly plausible that the core is formed via a VLS process and the shell is formed by a conformal growth process.

In Fig. 4(c), the Ge composition of the peripheral region is almost constant from the bottom to the top except for position 1, where the shell is very thin. This result suggests that the Ge composition of the shell is close to being uniform. The thickness of the shell can easily be estimated from the shape of the SiGeNWs under the assumption that the diameter of the core is the same as that of the Au catalyst. The rate of conformal growth can be obtained from the shell thickness. In the case of the SiGeNW in Fig. 4, the conformal growth rate of the shell is about 2% of the VLS growth of the core. The conformal growth rate increases as $GeH_4/(GeH_4+Si_2H_6)$ increases, resulting in a more conelike shape, as can be seen in Fig. 1.

In position 6 in Fig. 4(a), the core diameter is about 76 nm, while the shell thickness is about 110 nm. If we average the Ge composition of the shell (~50 at %) and the core (~35 at %) by taking into account these core and shell sizes, the result is about 46 at %. This value is very close to that obtained at the central region of position 6. The same estimations made from positions 2 to 6 were able to reproduce the diameter dependence of Ge composition in the center region [Fig. 4(c)] within an accuracy of 10%. The agreement indicates that the Ge composition within the core, as well as that within the shell, tends to be uniform.

Figure 5 shows HRTEM images of an as-grown SiGeNW grown under the same conditions as those in Fig. 4. Figures 5(a) and 5(b) correspond to the top (catalyst side) and the bottom (substrate side) of the SiGeNW. Lattice

Author complimentary copy. Redistribution subject to AIP license or copyright, see http://jap.aip.org/jap/copyright.jsp

fringes correspond to the (111) planes of the $Si_{1-x}Ge_x$ alloy. We can see that the SiGeNW is defect-free single crystal from the bottom to the top, i.e., both the core grown by a VLS process and the shell by conformal growth are single crystals.

The growth of conelike core-shell type SiNWs with higher B concentration in the shell was reported in previous work on B-doped SiNWs.[15] The formation of these conelike shapes could also be explained by the enhancement of conformal growth under high B_2H_6 concentration growth conditions. However, in that case, the high B-concentration shell was not a single crystal but a highly defective polycrystal.[16] The formation of a polycrystal shell is also reported in VLS growth SiGeNWs.[8] Therefore, the shell of core-shell type Si-based NWs is not necessarily a single crystal, but the crystallinity depends on the growth condition.

As shown in Fig. 5, in the present SiGeNWs, a single crystal shell is epitaxially grown on the core. The growth of a single crystal shell in the present growth condition is understandable by considering the fact that uncatalyzed epitaxial growth of $Si_{1-x}Ge_x$ alloy thin films is possible under the present growth parameters. Epitaxial growth at fairly low temperatures (~450 °C) is partly due to the choice of Si source gas, Si_2H_6, the thermal stability of which is lower than that of the more commonly used SiH_4. The lower thermal stability decreases the lowest possible growth temperature and increases the growth rate. In fact, at a growth temperature of 500 °C, the growth rate of a Si film from Si_2H_6 is more than 20 times faster than that from SiH_4. The addition of GeH_4, the thermal stability of which is even lower than that of Si_2H_6, further decreases the lowest possible growth temperature and increases the growth rate. At a growth temperature of 500 °C, the growth rate of a $Si_{1-x}Ge_x$ film is about 7 nm/min when $x=0.25$, while it increases to 13 nm/min when $x=0.3$. The high growth rate of a $Si_{1-x}Ge_x$ film at a low growth temperature without catalysts results in the formation of a single crystal $Si_{1-x}Ge_x$ shell on the surface of the SiGeNWs.

C. Effects of oxidation

For some device applications of SiGeNWs, the formation of a SiO_2 layer on the surface is required. We thus studied the effects of oxidation on the structure and Ge composition of SiGeNWs. Figure 6 shows Raman spectra of SiGeNWs before and after oxidation at different temperatures for 2 min. The Ge composition of the as-grown SiGeNWs, estimated from Eq. (1), is 0.21. The small Ge composition results in small intensities of Si-Ge and Ge-Ge modes. These modes grow significantly by oxidation at 900 °C. By further increasing the oxidation temperature, they grow further, and all the modes are broadened. When the oxidation temperature is 1100 °C, the Ge-Ge mode splits into two peaks. The existence of two different frequency Ge-Ge modes indicates that two different Ge composition regions are formed in the SiGeNWs.

We attempted to estimate the Ge composition of oxidized SiGeNWs using the same procedure as employed for the as-grown ones. However, the values estimated from Eqs.

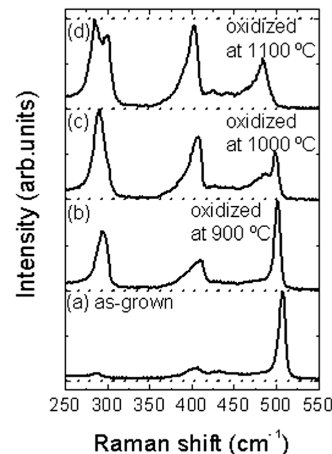

FIG. 6. Raman spectra of as-grown and oxidized SiGeNWs. (a) as-grown; (b), (c), and (d) oxidized at 900, 1000, and 1100 °C, respectively, for 2 min. The ratio of partial pressures of GeH_4 and Si_2H_6 $[GeH_4/(GeH_4+Si_2H_6)]$ is 0.6 and that of H_2 is 1100 sccm. Growth temperature is 450 °C and growth duration is 10 min.

(1)–(3) are very much scattered, preventing this method from being applied to oxidized SiGeNWs. To demonstrate how much the estimated values were scattered, we plotted the intensity ratio of the Ge-Ge and Si-Si modes as a function of Ge composition in Fig. 3(b). As before, the symbols are the Ge composition estimated from Eq. (1); and the error bars correspond to those estimated from Eqs. (2) and (3). The solid curve is the same as that shown in Fig. 3(a). The data for the samples with $GeH_4/(GeH_4+Si_2H_6)$ of 0.6 and the growth temperatures of 350 °C (open symbols) and 450 °C (filled symbols) are shown. The oxidation temperatures are 900 °C (○●), 1000 °C (△▲) to 1100 °C (□■). Since there are two Ge-Ge peaks in the sample oxidized at 1100 °C, two data are simultaneously shown for the sample. It is clear that oxidation significantly increases the intensity ratio and the error bars in the abscissa become extremely large. These results suggest that segregation of Ge occurs and SiGeNWs become very inhomogeneous. It is noted that Eqs. (1)–(3) are valid in the x range of 0–0.5, and for $x>0.5$ different relations are used.[17] For some oxidized samples with high intensity ratios of the Ge-Ge and Si-Si modes, we try to estimate x by the relations applicable to the higher Ge composition ranges. However, the x values do not change significantly from those estimated from Eqs. (1)–(3).

To confirm the above discussion, we performed TEM observations of oxidized SiGeNW (Fig. 7). The oxidation temperature and duration are 1100 °C and 4 min, respectively. We can see the growth of a SiO_2 layer about 25 nm in thickness by oxidation. At the interface between the SiO_2 layer and the SiGeNW, 5–15 nm particles are seen. TEM-EDS analyses revealed that these particles are composed mainly of Ge atoms. We also found that the Ge composition in the SiGeNW increases after oxidation.

In the oxidation of $Si_{1-x}Ge_x$ thin films, Si is preferentially oxidized and Ge atoms are piled up at $SiO_2/Si_{1-x}Ge_x$ interfaces. This causes the formation of Ge particles at the interface, and inhomogeneity in the composition of the remaining $Si_{1-x}Ge_x$ layer.[18] Similarly, in the oxidation of SiGeNWs, segregation of the Ge atoms at the interface be-

Author complimentary copy. Redistribution subject to AIP license or copyright, see http://jap.aip.org/jap/copyright.jsp

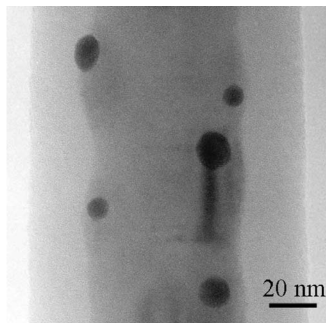

FIG. 7. TEM image of a SiGeNW after oxidation at 1100 °C for 4 min. The ratio of partial pressures of GeH_4 and Si_2H_6 $[GeH_4/(GeH_4+Si_2H_6)]$ is 0.78 and the growth temperature is 450 °C.

tween the SiGeNW core and SiO_2 shell leads to inhomogeneity of the Ge composition, as can be seen in Fig. 3(b). The present results indicate that great care should be taken in oxidizing SiGeNWs. Under the present oxidation conditions, oxidation is faster than the diffusion of piled-up Ge atoms toward the NW core. To avoid the formation of Ge particles and minimize the inhomogeneity, SiGeNWs should be oxidized at a lower rate by keeping the Ge diffusion rate high. This can be achieved by oxidizing SiGeNWs in a diluted oxygen gas atmosphere. To confirm this, we oxidized SiGeNWs in atmospheres of 1% O_2 in N_2 and 10% of O_2 in N_2. In these atmospheres, no splitting of the Ge-Ge Raman mode was observed, even when fairly high Ge composition samples (x=0.2–0.3) were oxidized at 1100 °C.

In discussing the Raman spectra, we did not take into account the effect of strain at the core/shell interfaces, SiO_2/SiGeNWs interfaces, Ge particle/SiGeNWs interfaces, etc. In as-grown SiGeNWs, the effect of strain seems to be not very large because the Raman data can be fully explained by the stress-free empirical relations in Eqs. (1)–(3). On the other hand, in oxidized SiGeNWs, strain and its distribution is considered to be one of the reasons for the large scattering of Raman data in Fig. 3(b). However, unfortunately, at the present stage of research we cannot distinguish between the distributions of Ge composition and that of strain.

IV. CONCLUSIONS

SiGeNWs grown by UHV-CVD were studied in detail by Raman spectroscopy, TEM, and TEM-EDS. By systematically changing the growth conditions over a wide range, we clarified the relationship between the growth parameters and the structure of SiGeNWs. Our Raman and TEM-EDS results demonstrated that SiGeNWs consist of a lower Ge composition single crystal core grown via Au catalysts and a higher Ge composition single crystal shell epitaxially grown on the core. The TEM-EDS results revealed that the Ge composition within the core and the shell is almost constant. We also studied the effects of oxidation on the structure of SiGeNWs and showed that oxidation leads to segregation of Ge atoms at the interface between the SiGeNWs and SiO_2, which in turn results in a large inhomogeneity in Ge composition. We believe oxidation at a very low rate in a diluted oxygen gas atmosphere to be effective in preventing the formation of Ge particles and minimizing any inhomogeneity.

ACKNOWLEDGMENTS

The authors thank Mr. Tatsunori Mizutani of Matsushita Technoresearch for the TEM measurements. The authors thank Mr. Hiroyuki Masuda, Dr. Tohru Nakagawa, Dr. Hideo Torii, and Mr. Sadayoshi Hotta for the experimental support and discussions on this work. This work was supported by a Grant-in-Aid for Science Research from the Ministry of Education, Science, Sports, and Culture of Japan.

[1] Y. Cui, Z. Zhong, D. Wang, W. U. Wang, and C. M. Lieber, Nano Lett. **3**, 149 (2003).
[2] M. C. McAlpine, R. S. Friedman, S. Jin, K. Lin, W. U. Wang, and C. M. Lieber, Nano Lett. **3**, 1531 (2003).
[3] Y. Cui, Q. Wei, H. Park, and C. M. Lieber, Science **293**, 1289 (2001).
[4] J. Hahm and C. M. Lieber, Nano Lett. **4**, 51 (2004).
[5] X. Duan, Y. Huang, R. Agarwal, and C. M. Lieber, Nature (London) **421**, 241 (2003).
[6] M. H. Huang, S. Mao, H. Feick, H. Yan, Y. Wu, H. King, E. Weber, R. Russo, and P. Yang, Science **292**, 1897 (2001).
[7] Y. Wu, R. Fan, and P. Yang, Nano Lett. **2**, 83 (2002).
[8] K. Mori, K. Shoda, and H. Kohno, Appl. Phys. Lett. **87**, 083111 (2005).
[9] J. C. Tsang, P. M. Mooney, F. Dacol, and J. O. Chu, J. Appl. Phys. **75**, 8098 (1994).
[10] M. I. Alonso and K. Winter, Phys. Rev. B **39**, 10056 (1989).
[11] P. M. Mooney, F. H. Dacol, J. C. Tsang, and J. O. Chu, Appl. Phys. Lett. **62**, 2069 (1993).
[12] S. M. Jang, K. Liao, and R. Reif, J. Electrochem. Soc. **142**, 3513 (1995).
[13] Y. Miyamoto and M. Hirata, Jpn. J. Appl. Phys. **14**, 1419 (1975).
[14] K. Lew, L. Pan, E. C. Dickey, and J. M. Redwing, Adv. Mater. **15**, 2073 (2003).
[15] E. Tutuc, S. Guha, and J. O. Chu, Appl. Phys. Lett. **88**, 043113 (2006).
[16] T. Kawashima, G. Imamura, T. Saitoh, K. Komori, M. Fujii, and S. Hayashi, J. Phys. Chem. C **111**, 15160 (2007).
[17] S. Gu, L. Qin, R. Zhang, and Y. Zheng, Appl. Phys. A: Mater. Sci. Process. **62**, 387 (1996).
[18] Y. S. Lim, J. S. Jeong, J. Y. Lee, H. S. Kim, H. K. Shon, H. K. Kim, and D. W. Moon, Appl. Phys. Lett. **79**, 3606 (2001).

Author complimentary copy. Redistribution subject to AIP license or copyright, see http://jap.aip.org/jap/copyright.jsp